

2  
3  
**Particle tracking velocimetry applied to thermal counterflow  
in superfluid  $^4\text{He}$ : Motion of the normal fluid at small heat fluxes**4 B. Mastracci, S. Bao, and W. Guo<sup>✉</sup><sup>\*</sup>5 *National High Magnetic Field Laboratory, 1800 East Paul Dirac Drive, Tallahassee, Florida 32310, USA*  
6 *and Mechanical Engineering Department, Florida State University, Tallahassee, Florida 32310, USA*

7 W. F. Vinen

8 *School of Physics and Astronomy, University of Birmingham, Birmingham B15 2TT, United Kingdom*

(Received 12 April 2019; published xxxxx)

10  
11 This paper is concerned with thermal counterflow in superfluid  $^4\text{He}$ , particularly with  
12 the motion of the normal component at small heat fluxes when this motion is believed to  
13 be laminar. Recent experiments in which this motion is traced with micron-sized particles  
14 of solid deuterium show that the motion is not spatially uniform on a scale of order the  
15 spacing of the quantized vortex lines in the superfluid component. It is argued that this lack  
16 of uniformity has its origin in the fact that the force of mutual friction, which limits the  
17 thermal conductivity, is concentrated near the cores of the vortex lines. Possible effects  
18 of this concentration of force are discussed, and it is concluded that the experimental  
19 observations can be explained only if the vortex lines are arranged randomly in space,  
20 so that the observed lack of uniformity in the normal-fluid velocity can be regarded as  
21 being due partly to spatial variations in the vortex line density. However, problems remain,  
22 in that the form of the observed velocity correlation function has still to be understood.23 DOI: [10.1103/PhysRevFluids.00.003300](https://doi.org/10.1103/PhysRevFluids.00.003300)24  
**I. INTRODUCTION**25  
26  
27  
28  
29  
30  
31  
32  
33  
34  
35  
36  
37  
38  
39  
40  
41 It has long been known that, according to the two-fluid model, heat is carried in superfluid  $^4\text{He}$  by  
a counterflow of the two fluids, the superfluid component flowing toward the source of heat and the  
normal component flowing away from it [1]. Such counterflow normally takes place in a channel,  
and in this paper we are concerned with a channel with cross-section of order 10 mm  $\times$  10 mm.  
Experiments over the years (see, for example, Refs. [2–4] and references therein) have shown that in  
such channels the characteristics of the counterflow change as the heat flux increases. At the smallest  
heat fluxes the superfluid component flows without friction, while the flow of the normal fluid is  
limited only by its viscosity. Over a range of somewhat larger heat fluxes the superfluid component  
becomes turbulent, in the sense that it supports a random tangle of quantized vortex filaments; the  
thermal excitations constituting the normal fluid are scattered by these filaments, giving rise to a  
force of “mutual friction” between the two fluids. This mutual friction can modify the (laminar)  
velocity profile in the normal fluid, especially at larger heat fluxes. Then as the heat flux increases  
still further there is a transition at which large-scale turbulence is established in both fluids, the two  
turbulent fields being partly coupled through the mutual friction, and large-scale turbulence in the  
superfluid component being achieved by partial polarization of the vortex filaments.The experiments to which we have just referred were based for the most part on observations  
with second sound, the attenuation of which allows measurement of vortex filament densities, and\*Corresponding author: [wguo@magnet.fsu.edu](mailto:wguo@magnet.fsu.edu)

42 with  $\text{He}_2$  excimer molecules, which trace the flow of the normal fluid. Particle tracking velocimetry  
 43 (PTV), using micron-sized particles of solid hydrogen or solid deuterium as tracers, has also  
 44 been used, as reviewed in a recent paper by Mastracci and Guo [5]. This paper also reports new  
 45 experimental results, which include information about the motion of the tracer particles that are  
 46 known to be tracking the motion of the normal fluid on length scales smaller than those easily  
 47 accessible to tracking by  $\text{He}_2$  excimer molecules (scales of order the spacing of the vortex filaments),  
 48 particularly at heat fluxes at which there is a random tangle of vortex filaments and laminar flow of  
 49 the normal fluid. In the present paper we discuss the interpretation of this observed motion.

50 At first sight it might be thought that when the flow of the normal fluid is laminar there ought to  
 51 be no small-scale motion. However, this would be true only if the force of mutual friction, which  
 52 is principally responsible for limiting the flow of the two fluids, were applied in a spatially uniform  
 53 manner. In reality, the force is applied to the normal fluid only very close to the cores of the vortex  
 54 filaments [6]; transfer to the bulk of the normal fluid takes place only through the viscosity of the  
 55 normal fluid. We shall argue that the resulting perturbation to the velocity field in the normal fluid  
 56 is responsible, at least in part, for the observed small-scale motion of the normal fluid.

57 The theoretical ideas in this paper are for the most part not new. The perturbation in the velocity  
 58 field in the normal fluid resulting from motion of a single vortex was recognized in Refs. [2,6], to the  
 59 extent that the effect was taken into account in a calculation of the actual magnitude of the mutual  
 60 friction; but the calculations in Refs. [2,6] did not require a knowledge of the perturbation at larger  
 61 distances from the lines. More recently Idowu *et al.* [7] carried out a numerical simulation of the  
 62 perturbation, which we shall discuss later (see also Refs. [8,9]). It turns out, however, that, as we  
 63 shall see, the probable perturbation in the normal-fluid velocity field by a single vortex is too small  
 64 to account for our experimental results. We show instead that spatial inhomogeneities in the density  
 65 of vortex lines are the probable cause of the observed effects, although the way in which these spatial  
 66 inhomogeneities operate is quite subtle and may not be fully understood. Indeed, a fully satisfactory  
 67 explanation must await a more sophisticated treatment than we are able to provide, and may involve  
 68 physical effects that we have not yet fully identified. To this extent the theory that we present must  
 69 be regarded as only a useful first step in understanding the experimental results that we present.

70 The theoretical problems underlying our experimental results will be explored in two steps. First,  
 71 we shall discuss in general terms the likely perturbation in the velocity field resulting from the  
 72 motion of a single rectilinear vortex. In essence this ought to involve an understanding of the way  
 73 in which the moving vortex drags the normal fluid in its vicinity. We present new calculations of  
 74 this dragging effect, arguing that those of Idowu *et al.* are inadequate. We conclude that dragging  
 75 by the individual vortices is insufficient to account for the experimental results. Our second step is  
 76 then to suggest that the experimental results can be understood only in terms of the way in which a  
 77 moving disordered array of vortices perturbs the velocity of the normal fluid. As we shall see, this  
 78 is in detail a difficult problem that requires new types of simulation, and we are able here to give  
 79 only an introductory discussion of it.

80 The relevant experimental results are summarized in Sec. II; they include results already  
 81 published in Ref. [5], together with some new results relating to the way that normal-fluid velocities  
 82 are correlated in time. The theoretical discussion is presented in Sec. III, and a summary is given in  
 83 Sec. IV. Details of the new calculation of the dragging by a single vortex are given in the Appendix.

## II. EXPERIMENTAL RESULTS

84 The apparatus used by Mastracci and Guo was described in detail in Ref. [5]. The heat flow took  
 85 place in a channel of 16-mm-square cross section. Tracks of deuterium particles were observed  
 86 and analysed at various temperatures and various steady counterflow velocities, and probability  
 87 distribution functions (PDFs) for the particle velocity were extracted.

88 In Fig. 1 we show typical PDFs for the streamwise component of the velocity (i.e., parallel to the  
 89 steady heat flux). As has been observed in previous studies, this PDF exhibits two peaks at low heat  
 90 fluxes [Fig. 1(a)], the peaks merging into a single peak at large heat fluxes [Fig. 1(b)]. Gaussian

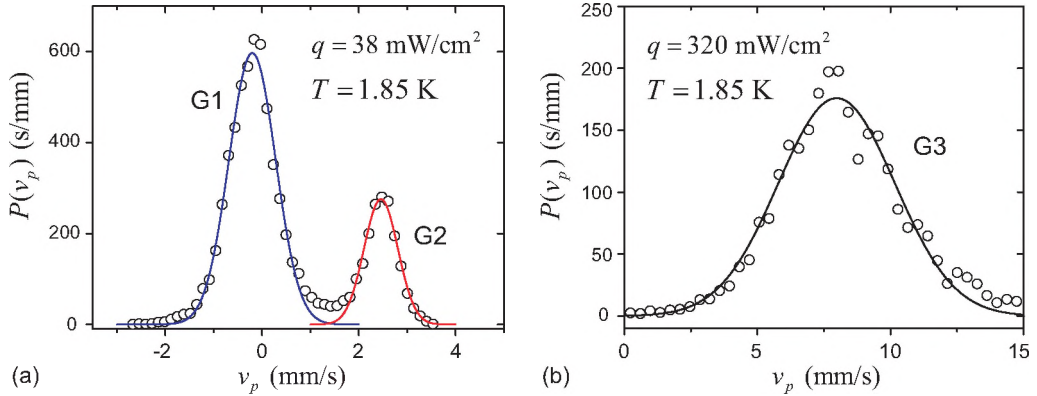


FIG. 1. The calculated streamwise particle velocity PDFs at 1.85 K for heat fluxes of 38 and 320 mW/cm<sup>2</sup>. The solid lines are Gaussian fits to the data.

fits to the peaks lead to corresponding mean velocities,  $\langle v_p \rangle$ , and velocity standard deviations,  $\Delta v_p = \langle (v_p - \langle v_p \rangle)^2 \rangle^{1/2}$ . In the two-peak regime the value of  $\langle v_p \rangle$  for the G2 peak agrees well with the expected mean velocity of the normal fluid ( $q/\rho ST$ ), so that we can identify this peak as being due to particles that are moving, at least on average and for a significant length of time, with the normal fluid. The G1 peak is due to particles that are trapped on vortices. At higher heat fluxes, when the two peaks merge,  $\langle v_p \rangle$  is observed to be equal to about half the steady normal-fluid velocity, and in this regime particles are, in rapid succession, being continually trapped on vortices and then released by viscous drag from the normal fluid. In this paper we are concerned only with the width (standard deviation) of the G2 peak, both for the streamwise velocity, which we have been discussing, and also for the velocity transverse to the steady normal-fluid flow.

In Fig. 2 we show these observed standard deviations as functions of the mean normal-fluid velocity,  $\langle v_n \rangle$ , at three temperatures. We see that the transverse velocity standard deviations are small and almost independent of  $\langle v_n \rangle$ , whereas the streamwise standard deviations show a marked increase. In fact, the former standard deviations are only a little larger than the effect of environmental noise. The streamwise standard deviations could well be proportional to  $\langle v_n \rangle$ , although the noise is too large to allow us to draw a definitive conclusion.

Our experimental results allow us to calculate not only these standard deviations, which were reported in Ref. [5], but also velocity correlation functions, which we report here for the first time,

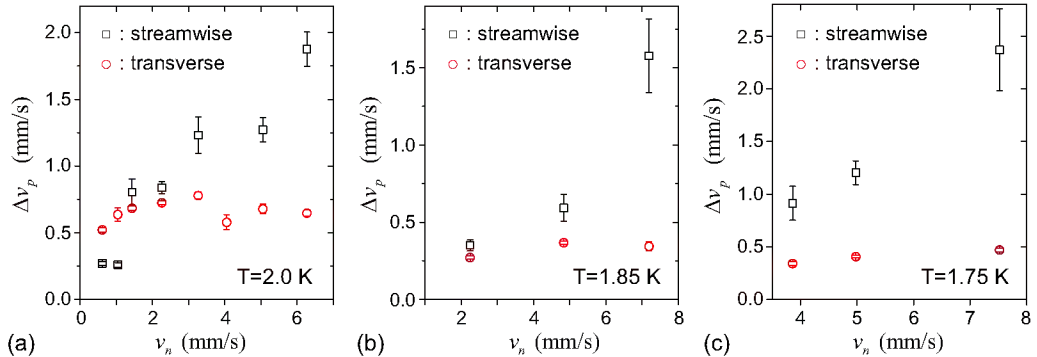


FIG. 2. Calculated streamwise and transverse velocity standard deviations for the G2 particles at three temperatures.

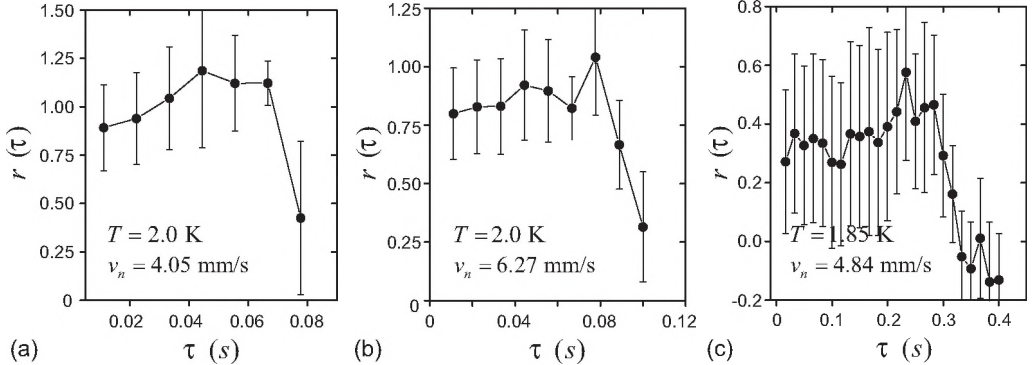


FIG. 3. Calculated streamwise velocity correlation functions for the G2 particles at different temperatures and heat fluxes.

110 and which are defined as

$$r(\tau) = \frac{\langle (v_p(t) - \langle v_p \rangle)(v_p(t + \tau) - \langle v_p \rangle) \rangle}{\Delta v_p^2}, \quad (1)$$

111 where  $v_p(t)$  is the velocity of a particular particle on a track measured at time  $t$ . These correlation  
 112 functions tell us the characteristic lifetimes of the velocity fluctuations, as seen by a particular  
 113 particle. Our observed values of  $r(\tau)$  for streamwise fluctuations under various conditions are  
 114 shown in Fig. 3. Owing to our limited sample sizes, our values of  $r(\tau)$  are subject to considerable  
 115 uncertainty, but there is little doubt that the lifetimes of the streamwise fluctuations are roughly  
 116 100 ms at a temperature of 2 K. But the precise way in which  $r(\tau)$  varies with  $\tau$  is less clear: It  
 117 may be more or less flat up to a point where there is an abrupt fall; or there may be a more gradual  
 118 fall. Our observations of correlation functions for transverse velocities show no interesting structure,  
 119 being dominated by noise. (We note that the observed  $r(\tau)$  appear not always to tend to unity as  $\tau$   
 120 tends to zero. This is probably due to the fact that our signals contain significant amounts of noise,  
 121 for which the correlation time is very small, leading to a fall in  $r(\tau)$  at unobservably small times.)

122 We have noted that the correlation functions are related to characteristic lifetimes of the normal-  
 123 fluid fluctuations, as seen by a particular particle. We have also noted that  $r(\tau)$  may be fairly flat,  
 124 until  $\tau$  reaches a value of  $\tau_c$ , when there is a fairly sharp cutoff in the correlation. If, as we are  
 125 suggesting, the fluctuations are due to local dragging of the normal fluid by vortex lines, and if we  
 126 assume for the moment that the vortex lines remain at rest in the frame of reference moving with  
 127 the average velocity of the superfluid, then in this frame of reference the flow of the normal fluid is  
 128 stationary and the characteristic length  $\zeta = (v_n - v_s)\tau_c$  is the distance in the streamwise direction  
 129 over which the dragging is effective. For the case depicted in Fig. 3(b)  $\zeta$  proves to be about 30 times  
 130 the average vortex-line separation. The magnitude of the perturbation in  $v_n$  at distances less than  $\zeta$   
 131 is of order  $\Delta v_p$  for the streamwise flow. If  $r(\tau)$  is roughly flat, for  $\tau < \tau_c$ , then this magnitude does  
 132 not depend strongly on distance for distances less than  $\zeta$ .

133 We note that the measurements that we have been describing serve to measure correlations in  
 134 the direction of the heat flux (i.e., longitudinal correlations). As we shall see more clearly later, it  
 135 would be interesting to measure also the transverse correlations. Such measurements are possible  
 136 in principle, but they require a study of the correlated motion of two particles. In our observations  
 137 so far the density of tracer particles has been too small to allow such study with adequate statistical  
 138 error.

139 In our Introduction we mentioned observations of the normal-fluid flow with  $\text{He}_2$  excimer  
 140 molecules. They involved the production of a narrow line of these molecules, perpendicular to the  
 141 heat flux, and an observation of the way in which this line changes as it moves with the normal fluid.

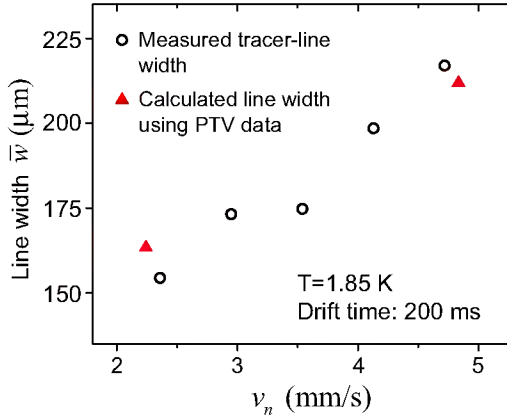


FIG. 4. The observed broadening of the excimer lines at 1.85 K with increasing normal-fluid velocity, when the flow of normal fluid is observed to be laminar. The red triangles show the broadening expected from the PTV results reported in this paper

Three types of change are possible: a broadening of the line owing to diffusion of the molecules; distortion of the line owing to turbulent or other forms of normal fluid motion on scales greater than the line width; and a further broadening owing to these forms of motion on scales less than the line width. We are arguing in this paper that when the normal-fluid flow is laminar there can still be nonuniformities in the velocity of the normal fluid on scales of order the spacing between vortex lines, these scales being less than the observed linewidths. Such nonuniformities ought therefore to contribute to the broadening of the lines of excimers, such broadening being probably proportional to the average normal-fluid velocity,  $v_n$ . Thus, if the lines are examined after they have drifted for a time  $t_{\text{drift}}$ , we may expect the line width,  $\bar{w}$ , to change with  $v_n$  according to the equation  $\bar{w} = \bar{w}_0 + At_{\text{drift}}v_n$ , where  $\bar{w}_0$  is the initial width enhanced by that due to diffusion during the drift time, and where the constant of proportionality,  $A$ , is known from the experiments described earlier in this section. The results of a recent careful analysis of our earlier experiments with excimers are shown in Fig. 4, where we have plotted the observed linewidth against  $v_n$  at 1.85 K for a fixed drift time and for heat fluxes at which flow of the normal fluid is observed to be laminar. The red triangles show that the broadening expected from the above equation agrees well with experiment.

### III. THEORETICAL DISCUSSION

#### A. Introduction

There appear to be three possible explanations of the observed fluctuations of the G2 particle velocities: that there is in fact small-scale turbulence in the normal fluid; that the velocity of G2 particles is occasionally perturbed by scattering from vortex lines; that the velocity of the normal fluid is perturbed by the frictional interactions with the vortex lines (dragging of the normal fluid).

Small-scale turbulence in the normal fluid seems possible, although it would need to be extremely anisotropic, with hardly any motion transverse to the counterflow; for reasons that will become clear later, we believe and argue that any such turbulence is not *fundamentally* responsible for the observed fluctuations. The second of the possible effects can be ruled out as follows. Scattering of a particle by a vortex line must involve a timescale of order  $\sigma/v_{G2}$ , where  $\sigma$  is the scattering cross-section and  $v_{G2}$  is the particle velocity (at this point we rule out any “scattering” that is really associated with dragging of the normal fluid [9]). This time is unlikely to be greater than about 10  $\mu s$ . But we know that the velocity of a tracer particle of radius  $a$  will recover from any perturbation in a time of order  $\rho a^2/3\eta_n$ , where  $\rho$  is the density of the helium and  $\eta_n$  is the viscosity of the normal

fluid [10]; this time is of order  $30 \mu\text{s}$ . These times are much smaller than the times over which the perturbed particle velocities are observed to persist.

As we suggested in our general introduction, we believe that the fluctuations in the G2 particle velocities are in fact due to dragging of the normal fluid induced by the frictional interaction with the discrete vortices. In the remaining part of this paper we shall first show that dragging by an individual vortex is too small to account for our observations; nevertheless, as far as we know, our treatment of this dragging is new and of some intrinsic interest, an earlier treatment by Idowu *et al.* [7] having been unsatisfactory. Then we shall show, with a simple model, that dragging by a disordered array of lines, such as is believed to be present in a counterflow, does lead to effects that are much larger; effects that could be, at least qualitatively, consistent with our observations. However, we are not able yet to account for the precise form of the correlation function displayed in Fig. 3, which remains a serious problem.

## B. The dragging of the normal fluid by an individual quantized vortex

The existence of this dragging effect was first recognized in Refs. [2,6], to the extent that the effect was taken into account in a calculation of the actual magnitude of the mutual friction; but the calculations in Refs. [2,6] did not require a knowledge of the perturbation at larger distances from the lines. Nevertheless it was suggested that the dragging could be explained rather fully as being similar to the dragging of an infinite classical viscous fluid at low Reynolds number by a thin solid cylinder moving at right angles to its length, especially not too close to the cylinder. This view is elaborated in an Appendix, where we use it to derive expressions for the perturbed velocity field in an infinite volume of normal fluid arising from the slow movement of a rectilinear vortex at velocity  $U$ . The character of this perturbation at a distance  $r$  from the vortex depends on the value of  $r$  relative to a characteristic length  $\lambda = v_n/2U$ , where  $v_n = \eta_n/\rho_n$  is the kinematic viscosity of the normal fluid. We have obtained expressions for the perturbation in terms of the force,  $f$ , of mutual friction per unit length of vortex in the limits of both  $\lambda \gg r \gg \xi$  (the “near field”) and  $r \gg \lambda$  (the “far field”); the length  $\xi$  is the range over which the force of mutual friction acts near the core of the vortex. It turns out that for the experiments described in Sec. II  $\lambda$  is much smaller ( $\sim 0.7 \mu\text{m}$ ) than the distances over which the normal-fluid velocity is observed to be perturbed, so that we need focus only on the far velocity field, given by Eq. (A7).

Our experimental results, described in Sec. II, relate to thermal counterflow. For the present it is sufficient for us to assume that the vortex of interest moves with the average velocity of the superfluid component, so that we can take  $U = \langle v_s \rangle - \langle v_n \rangle = (\rho/\rho_s)\langle v_n \rangle$ , where  $\rho$  is the density of the helium and  $\rho_s$  is the density of the superfluid component. We note that the force of mutual friction,  $f$ , can be expressed in terms of  $U$  as  $\alpha\kappa\rho_s U$  (see Ref. [11]), so that

$$f = \alpha\kappa\rho\langle v_n \rangle, \quad (2)$$

where  $\alpha$  is a dimensionless mutual friction constant, and  $\kappa$  is the quantum of circulation ( $2\pi\hbar/m_4$ ); we ignore any transverse component of the mutual friction. It follows that the far velocity field can be written

$$u_r(y, z) = -\frac{\alpha\kappa\langle v_n \rangle}{\nu} \left( \frac{\lambda}{2\pi z} \right)^{1/2} \exp \left( -\frac{y^2}{8\lambda z} \right), \quad (3)$$

where  $\nu = \eta_n/\rho$ , and where we have omitted the small radial flow that ensures mass continuity. We note that this equation describes a laminar wake, the width of which increases as  $\sqrt{(8\lambda z)}$  and in which the velocity falls as  $z^{-1/2}$ .

To display the result of this calculation in a useful way, we introduce dimensionless parameters as follows:  $\tilde{u}_n(\tilde{y}, \tilde{z}) = u_n(y, z)/\langle v_n \rangle$ , and all length scales are divided by a relevant vortex spacing  $\ell$ , so that

$$\tilde{u}_n(\tilde{y}, \tilde{z}) = -\frac{\alpha\kappa}{\nu} \left( \frac{\tilde{\lambda}}{2\pi\tilde{z}} \right)^{1/2} \exp \left( -\frac{\tilde{y}^2}{8\tilde{\lambda}\tilde{z}} \right). \quad (4)$$

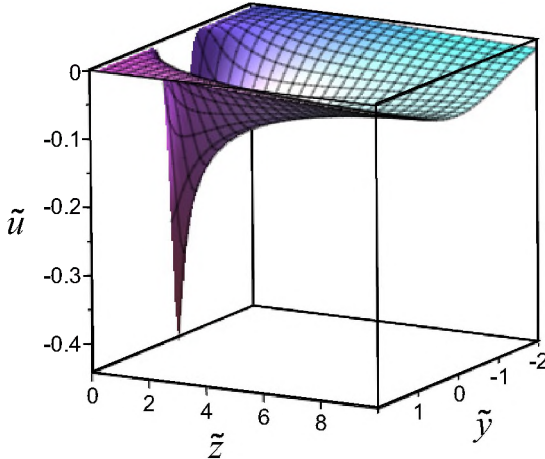


FIG. 5. The wake generated in the normal fluid by a single rectilinear vortex line.

For illustrative purposes we shall apply Eq. (4) to a counterflow at  $\langle v_n \rangle = 6 \text{ mm s}^{-1}$ , with a temperature of 2.0 K; values of the relevant parameters (taken from our own measurements or from Ref. [12]) are then:  $\ell = 46 \mu\text{m}$ ;  $v_n = 1.0 \times 10^{-8} \text{ m}^2 \text{ s}^{-1}$ ;  $\alpha = 0.279$ ;  $\rho_n/\rho = 0.553$ ;  $\lambda = 0.68 \mu\text{m}$ . The result is shown in Fig. 5. We note that this wake decays too rapidly with distance to account for the observations reported in Sec. II. We add that so far we have confined much of our theoretical study to temperatures close to 2 K, since it is only at these temperatures that we have satisfactory experimental results; in fact, however, the essential features of our results are not strongly temperature dependent.

At this point we must refer to work of Idowu *et al.* [7], which was also concerned with the dragging of the normal fluid by a single moving vortex. In some respects this work was more ambitious than the analysis that we have just outlined, in the sense that the motion of the vortex relative to the normal fluid was taken as due to a prescribed motion of the superfluid with a force of mutual friction between the vortex and the normal fluid. Calculations were based on a normal fluid that obeys the Navier-Stokes equation (including its nonlinear terms), with the force of mutual friction localized close to the core of the vortex. Instead of relying on analytical results, Idowu *et al.* obtained the normal-fluid velocity field from a two-dimensional direct numerical simulation, the vortex moving in a 1-mm computational square box, with periodic boundary conditions, the normal-fluid velocity field being recorded when the vortex is near the center of the box. For the most part the velocities with which the vortex moves (relative to the normal fluid) were smaller than those relevant to our present studies and in the range of roughly 0.1 to 1  $\text{mm s}^{-1}$ . These velocities correspond at temperatures near those that we have investigated to values of  $\lambda$  that are significantly larger than our own; at 0.1  $\text{mm s}^{-1}$ ,  $\lambda \sim 100 \mu\text{m}$ , while at the larger velocity  $\lambda \sim 10 \mu\text{m}$ . This means that within the 1-mm computational box any wake would not be well developed, although it ought to be visible at the higher velocity. Nevertheless, no wake seems to have been formed in these simulations. More seriously, the characteristic length  $\lambda$  seemed to play no role, the form of the velocity field at all distances from the vortex being in that sense very different from that described by us. The velocity field obtained by Idowu *et al.* does seem to involve a characteristic length, as indicated in their Fig. 3, but, unlike  $\lambda$ , this length seems to be independent of the velocity with which the vortex moves relative to the normal fluid, except perhaps at temperature very close to the  $\lambda$  point. It is not clear what determines this characteristic length.

Doubts about the validity of these simulations arise for at least two reasons: the computational box was too small in relation to the spatial extent of the perturbed velocity field; and insufficient time was allowed for a steady state to be achieved. As we understand it, the velocity fields were

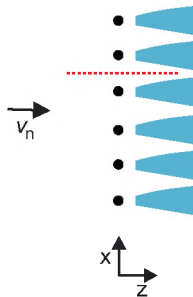


FIG. 6. Illustrating the effect of the small radial flows.

248 all observed at a time,  $t$ , equal to one second after the vortex was set in motion. At this time the  
 249 vorticity generated by motion of the vortex can have suffered viscous diffusion to a distance of only  
 250  $\delta = (2\eta_n t / \rho_n)^{1/2}$ , which is equal to only 0.19 mm, and which is therefore less than the size of the  
 251 computational box. This suggests that a steady state had not been reached, and that  $\delta$ , rather than  $\lambda$ ,  
 252 might be the characteristic length underlying the computations.

253 These considerations do of course raise the question whether a steady state is reached in  
 254 the experiments. It turns out that for practical purposes the steady state is reached, because the  
 255 characteristic length  $\lambda$  is much smaller than in the simulations of Ref. [7]. Therefore, our conclusion  
 256 about the perturbation of the normal fluid velocity caused by dragging by a single vortex still holds.  
 257 We must therefore seek another explanation for the experimental results of Sec. II.

258 We know from the success of simulations of counterflow turbulence in the superfluid component  
 259 that the vortex lines form at any instant a disordered array. This implies that the local density of  
 260 vortex lines, and hence the corresponding local value of the mutual friction, is nonuniform. This  
 261 nonuniformity will give rise to local variations in the velocity of the normal fluid, additional to  
 262 those already discussed, as is observed. To see whether these local variations might be sufficiently  
 263 large, we have tried to analyze the effect of a disordered array of rectilinear vortices. We shall  
 264 assume that each such vortex produces a wake, as described above. After the next section, which  
 265 aims to clarify how mass continuity is achieved with an array of vortices, we shall first discuss the  
 266 relationship between disordered wake structures and the velocity correlation functions introduced in  
 267 Sec. II; then we describe our calculated wake structures for disordered vortex arrays; and finally we  
 268 calculate velocity correlation functions for these disordered vortex arrays and compare them with  
 269 experiment.

### 270 C. Mass continuity in a moving vortex array

271 Before we describe these results with disordered arrays of vortices, we think it useful to enlarge  
 272 on the effect of the small radial flows described by the second term on the right-hand side of  
 273 Eq. (A7). As we have already explained, for the case of a single isolated rectilinear vortex, this term  
 274 serves simply to ensure mass continuity; there is an effective flow towards the vortex in the wake,  
 275 and the second term describes a consequential flow away from the vortex. However, it is less clear  
 276 how mass continuity is maintained in the case of an array of vortices, as we now explain. Consider,  
 277 for example, the flow of normal fluid past an infinite row of vortex lines, each line being normal to  
 278 the  $xz$  plane, as shown schematically in Fig. 6, the flow being maintained by a suitable temperature  
 279 gradient. In addition to the wakes (shown in blue), each vortex will produce a radial flow, away  
 280 from the vortex. Components of these radial flows in the direction of  $x$  will largely cancel, but let  
 281 us consider the effect of those in the direction of  $z$  along a line such as that shown broken in red.  
 282 They will serve first to decelerate the flow of the normal fluid for  $z < 0$  and then to accelerate it for  
 283  $z > 0$ . The deceleration will be canceled by the temperature gradient that is driving the flow of the  
 284 normal fluid, but the acceleration for  $z > 0$  serves to ensure that the total mass flow across a plane

$z = \text{constant}$  to the right of the vortices is conserved in spite of the smaller velocity existing within the wakes. Similar considerations apply to the disordered arrays that we now discuss.

#### D. Relations between disordered wake structures and velocity correlation functions

As we have stated, the vortices present in a thermal counterflow form a disordered array, and we must first consider how the corresponding wake structures are related to the observed velocity correlation functions described in Sec. II.

We work with cartesian coordinates  $(x, y, z)$ , the average steady velocity of the normal fluid being along the  $+z$  axis. We suppose that we have calculated the wake structure in the region  $z > 0$  due to all the vortices, forming a disordered array, in the region  $z \leq 0$ , and we denote the corresponding velocity field in the region  $z > 0$  by  $v(\text{wake}, z)$ . In addition there is in the region  $z > 0$  the velocity field  $v(2, z)$  due to the vortices in this region. Observation of the velocity correlation function serves to measure  $\langle (v(\text{wake}, 0)[v(\text{wake}, z) + v(2, z)]) \rangle$ . In what follows we shall assume that  $v(\text{wake}, 0)$  and  $v(2, z)$  are uncorrelated. This assumption seems reasonable if the disorder is sufficiently strong, and if we are dealing with arrays of parallel rectilinear vortices. In practice it is unlikely to be strictly correct, especially for more realistic configurations of vortices; but it is the best we can do at present. It means that the observed correlation function serves to measure  $\langle (v(\text{wake}, 0)(v(\text{wake}, z))) \rangle$ , which is obtained by suitable averaging of the wake structures discussed in the next section.

#### E. The velocity induced in the normal fluid by a disordered arrays of quantized vortex lines moving with the superfluid

Our aim in this section is to consider as best we can at this stage the perturbation in the velocity of the normal fluid caused by a disordered array of vortices, such as exists in a counterflow associated with a heat flux. We shall consider first the effect of a disordered array of parallel rectilinear vortices, aligned along the  $y$  axis in a Cartesian coordinate system, and stationary in the frame of reference moving with the average superfluid velocity.

We shall assume that the temperature and other parameters are the same as those relating to Fig. 5. Using a random number generator, we place 300 rectilinear vortices at random positions within the region defined by  $-10 < z/\ell < 0$ ,  $-15 < x/\ell < 15$ ; the positions of the central third of the vortices are shown in Fig. 7. We then calculate the total perturbation to the normal-fluid velocity in the region defined by  $0 < z/\ell < 50$ ,  $-5 < x/\ell < 5$ , assuming that the wakes are additive. This last assumption is justified because the Oseen equation, on which our simulations are based, is linear in the velocity perturbation  $u$ . The result is shown in Fig. 8(a). The result for a different set of random positions is shown in Fig. 8(b).

We see that the randomly positioned rectilinear vortices lead to random perturbations in the normal-fluid velocity that are quite large and extend to distances that are much greater than those generated by a single vortex. Perturbations that vary slowly in the transverse direction seem to decay more slowly in the direction of flow, and can decay in distances greater than  $50\ell$ , although perturbations that vary more rapidly in the transverse direction tend to decay in distances of order  $10\ell$ . The fact that the predicted perturbations in the normal-fluid velocity extend much further than those due a single vortex suggests that we may be on the right lines to account for the experimental results of Sec. II. However, we have still to calculate and display the form of the expected correlation function that can be compared with the experimental data in Fig. 3, and we shall do this in the next Section.

As is clear from Figs. 8(a) and 8(b), the width of the region where the normal-fluid velocity is perturbed depends on the particular random arrangement of the vortices. We have already noted that, although such widths are in principle measurable, they cannot be deduced with adequate accuracy from our existing observations.

Although the large perturbations in normal-fluid velocity that we see in our simulations must arise from inhomogeneities in the density of vortex lines, we can see no simple connection with the

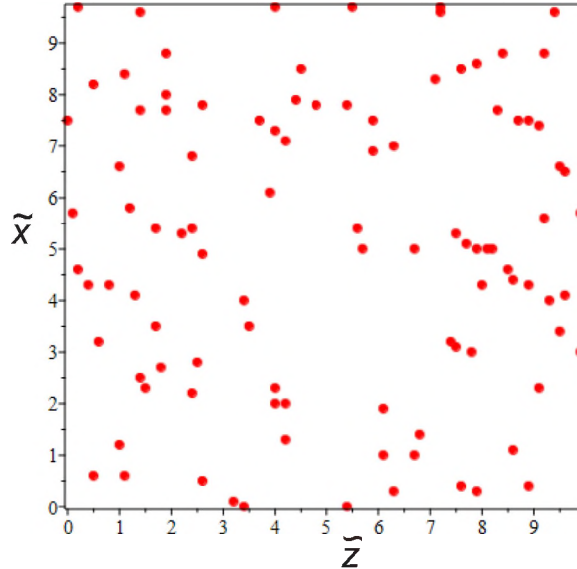


FIG. 7. Rectilinear vortices in random positions.

333 spectrum of vortex density fluctuations, which has been the subject of a good deal of study (see, for  
 334 example, Refs. [13,14]).

335 We must emphasize that our theoretical analysis so far has ignored the motion of the vortex  
 336 lines relative to the average superfluid velocity, and we shall attempt to address this deficiency in  
 337 Sec. III(g).

338 Before we embark on the next section we mention briefly that we have also investigated the  
 339 perturbations in the normal fluid velocity produced by a random arrangement of vortex rings at  
 340 a temperature of 2 K, the density of the rings being such that the line densities are similar to

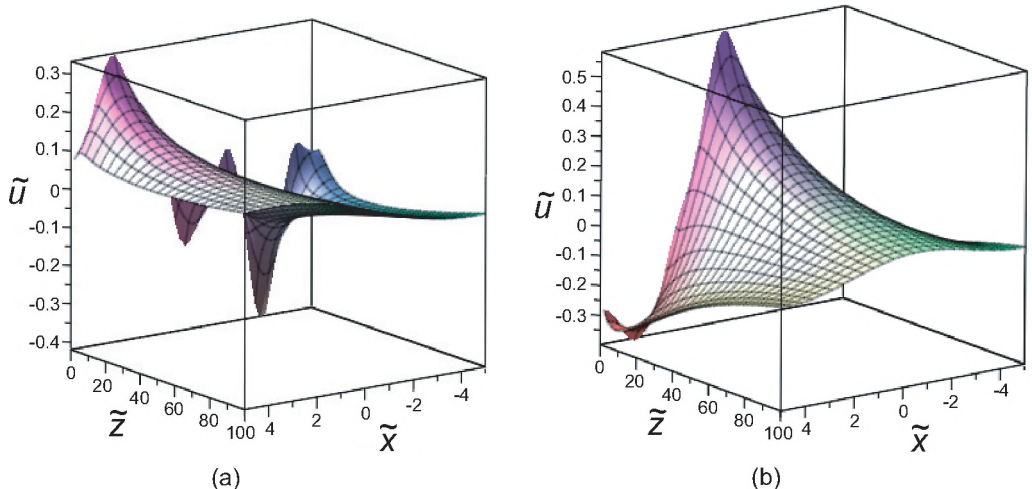
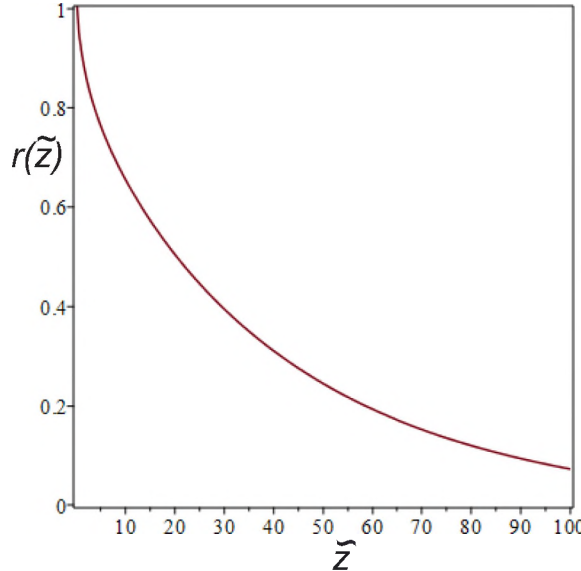


FIG. 8. (a, b) The wakes generated in the normal fluid by a randomly spaced array of rectilinear vortices; the dimensionless velocity in the wakes as a function of  $\tilde{x}$  and  $\tilde{z}$ . Figure 8(a) relates to the distribution of vortices in Fig. 7.

FIG. 9. The calculated correlation function,  $r(\tilde{z})$ , plotted against  $\tilde{z}$ .

those involved in our studies of random arrangements of rectilinear vortices. The results are broadly similar to those obtained with rectilinear vortices, suggesting that the results are not very sensitive to the precise arrangement of the vortices. Nevertheless, we recognize that we have not yet based our simulations on realistic vortex configurations.

#### F. Predicted form of the correlation function [Eq. (3)]

In accord with the argument in Sec. III(d), velocity fields of the type displayed in Fig. 8 can be used to calculate the correlation function  $r(\tilde{z})$ , which is equivalent to the correlation function  $r(\tau)$  introduced in Sec. II if we put  $\tau = \ell\tilde{z}/\langle v_n \rangle$ . The result, based on sets of data of the type displayed in Fig. 8 is shown in Fig. 9.

Comparing this calculated correlation function with its experimental counterpart (Fig. 3), we see that the ranges (in time or distance) are in approximate agreement, but that the forms of the function are not. At the present time we do not know the reason for this disagreement. Our assumption that the vortices are arranged in a completely random way may be wrong, and the fact that our vortex configurations are unrealistic may also be relevant. However, it seems unlikely that our calculations are misleading to such an extent that they lead to a correlation function that is so different in form from that suggested by experiment: i.e., from a rather strange form in which there is almost complete correlation over a time during which the tracing particle has moved a distance much greater than the average spacing between the vortex lines, followed by a rather abrupt fall. But these experimental data are, as we have already emphasized, subject to considerable uncertainty, so that we are led to the conclusion that they need to be subject to further careful checking.

In spite of these reservations, there seems little doubt that disordered arrays of vortex lines in the superfluid component in a thermal counterflow must lead to substantial inhomogeneities ( $\sim 30\%$ ) in the normal-fluid velocity, as is observed. It seems likely that any adequate theory of thermal counterflow ought to take account of these inhomogeneities, which has not so far been the case. Judging from the effect of a local reduction in the velocity of the normal fluid when it is associated with a normal fluid velocity profile in a channel of finite width [15], we guess that the inhomogeneities in this velocity discussed here are likely also to result in a significant inhomogeneities in the local vortex line density.

369 There is one apparently possible, but very speculative, explanation of the observed correlation to  
 370 which we ought briefly to refer. The irregular flow of the normal fluid that underlies the correlation  
 371 function displayed in Fig. 9 is essentially laminar, since it is derived from a superposition of  
 372 laminar wakes. However, an effective Reynolds number for this flow, formed from the mean velocity  
 373 fluctuations and the mean vortex spacing, is typically about 10, which suggests that a transition to  
 374 turbulent flow might occur on scales a little larger than the vortex spacing. It might be thought  
 375 that this turbulent flow would be significantly less anisotropic than the laminar flow, leading to  
 376 disagreement with experiment. However, a recent theoretical study [16] has shown that this might  
 377 not be the case. As we mentioned in our Introduction, it is now well-established that at heat fluxes  
 378 greater than those involved in the present study there is large-scale, partly coupled, turbulence in the  
 379 two fluids, in addition to the small-scale tangled motion of the vortex lines that has been the basis of  
 380 our discussion here [3]. The study in Ref. [16] shows that this large-scale motion is quite anisotropic,  
 381 especially on a small scale, the anisotropy arising from mutual friction because the turbulent eddies  
 382 in each fluid are being continually pulled apart in the direction of the steady relative motion of  
 383 the two fluids. The possibility exists therefore that a transition to turbulence in our case, which  
 384 would involve only small-scales but would still be in the presence of a steady counterflow, would  
 385 also preserve the anisotropy, especially if it were to involve partially coupled turbulence in both  
 386 fluids. Such a turbulent flow might possibly lead to a correlation function similar to that observed.  
 387 However, the arguments in Ref. [16] were based on continuum approximations to the flow of the  
 388 superfluid component, and it is very doubtful whether they can apply on scales only a little larger  
 389 than the vortex spacing. Furthermore, this small-scale turbulence could well be too strongly damped  
 390 by mutual friction. It should be emphasized that, even if this small-scale turbulence were indeed to  
 391 be established, it would still fundamentally have its origin in the local dragging of the normal fluid  
 392 by the vortex cores.

393 The development of a better theory poses major problems. Such a theory must probably be based  
 394 on simulations that take account of realistic vortex configurations interacting realistically with the  
 395 normal fluid. Such a theory must probably be based on simulations in which both the normal fluid  
 396 and the superfluid velocity fields are treated fully as coupled systems, as was done recently in a  
 397 different context by Yui *et al.* [17], and must take account of the time-dependence of the vortex  
 398 configurations (to which we refer in the next section). However, the spatial resolution required in  
 399 the normal fluid velocity needs to be better than the vortex line spacing,  $\ell$ , and therefore significantly  
 400 better than that in the simulations of Yui *et al.* At the same time there is a clear need to improve the  
 401 experimental observations, especially of the normal-fluid velocity correlation function.

402 **G. The effect of vortex lifetimes and of the random motion of the vortices relative  
 403 to the average superfluid velocity**

404 So far we have assumed in our model calculations that the vortices are not being continually  
 405 generated and destroyed in the thermal counterflow, and that they are at rest relative to the average  
 406 velocity of the superfluid component.

407 We note first that the vortices are moving in a random fashion, and that the corresponding random  
 408 vortex velocity can be obtained, at least to a reasonable approximation, from the local induction  
 409 approximation as follows [11]

$$v \sim \frac{\kappa}{4\pi R} \ln \left( \frac{R}{\xi_0} \right), \quad (5)$$

410 where  $\xi_0$  is the vortex core parameter, and where the mean value of  $1/R^2$  is given by

$$\left\langle \left( \frac{1}{R^2} \right) \right\rangle = c_2^2 \ell^{-2}, \quad (6)$$

where  $c_2$  is a constant equal to about 2. It follows that

$$v \sim \frac{c_2 \kappa}{\ell}. \quad (7)$$

As a result of this random vortex motion the arrangement of vortices develops in time, the characteristic time required for a significant change in this arrangement being given by

$$\tau_e = \frac{\ell^2}{c_2 \kappa}. \quad (8)$$

This random motion gives rise through mutual friction to dissipation [11,18], which is characterised by a time constant given by

$$\tau_D = \frac{2\pi}{\chi_2 \kappa L} = \frac{2\pi \ell^2}{\chi_2 \kappa}, \quad (9)$$

where  $\chi_2$  is a dimensionless parameter equal to about 3.5 at a temperature of 2 K [18]. The time constants  $\tau_e$  and  $\tau_D$  are similar in magnitude, and either can be taken as defining the timescale over which the arrangement of the vortices evolves. Using the numerical values set out in Sec. III(b), we find that this timescale is about 38 ms at 2 K. We emphasize that this timescale relates to vortex rearrangements on scales of order the vortex spacing; rearrangements on larger scales might well take place more slowly.

Vortex rearrangements could, to take two extreme cases, either generate wiggles on a normal-fluid wake or lead to the effective termination of the wake. The observed wakes seem to be characterized by a timescale of about 100 ms. It is not yet completely clear whether this time scale reflects the particular forms of vortex line inhomogeneities (so that, as we have assumed in earlier sections, it is not determined by random motion of the vortices), or whether it is determined by time-dependent vortex rearrangements. In any case it seems to be somewhat larger than 38 ms, although not necessarily much larger. As we have just emphasized, rearrangement on scales larger than the vortex spacing could take longer than 38 ms, and this does indeed appear to be the case. Further progress requires more sophisticated simulations than we are able to carry out, such as those of Yui *et al.*, to which we have already referred [17]. We note that wiggles on the wakes might account for the small transverse standard deviations shown in Fig. 2.

We must refer at this point to the work of Sergeev *et al.* [9]. They calculated the trajectories of micron-sized tracer particles interacting with the normal-fluid velocity field near a single moving rectilinear vortex line, expressing their results in terms of scattering cross-sections. As it turns out, this work is probably not directly relevant to the experimental results described in Sec. II, because, as we now see it, irregular motion of such tracer particles in a thermal counterflow is due more to nonuniformity in vortex density than to the dragging of normal fluid by an isolated vortex. As we have seen, the resulting irregular motion takes the form to a large extent of simply a spatial variation in the component of the drift velocity in the direction of the heat flux, without significant “scattering.”

#### IV. CONCLUSIONS

We have presented experimental results demonstrating that, even when the flow of the normal fluid is laminar, thermal counterflow leads to nonuniformity in the velocity of the normal fluid. Calculations are presented to show that probably this nonuniformity has its origin in the fact that the force of mutual friction is concentrated near the cores of the quantized vortex lines (an idea that is not new [2,6,7]), and that the characteristics of the observed nonuniformity can be produced only by a disordered arrangement of these lines. Although these calculations are in many ways unrealistic and based sometimes on questionable assumptions, we believe that they serve to capture the essential physics and are at least qualitatively correct. Further developments will require improved experimental data and more sophisticated theoretical analysis, as we have explained.

452 A depressing conclusion relates to the fact that existing simulations of thermal counterflow  
 453 turbulence (see, for example, Ref. [19]) do not take into account the effects that we describe and  
 454 may therefore be unreliable. An interesting, if speculative, conclusion is that the inhomogeneities in  
 455 the normal fluid velocity that we describe may be a precursor of the large scale coupled turbulence  
 456 that is observed to set in at heat currents a little larger than those relevant to our present studies [3].

## 457 ACKNOWLEDGMENTS

458 We are grateful for a helpful discussion with Carlo Barenghi in connection with the validity of  
 459 the simulations reported in Ref. [7]. B.M., S.B., and W.G. acknowledge the support from the U.S.  
 460 Department of Energy under Grant No. DE-SC0020113 for the PTV work and the support from the  
 461 National Science Foundation under Grant No. DMR-1807291 for the excimer tracer-line work. The  
 462 experiments were conducted at the National High Magnetic Field Laboratory, which is supported by  
 463 National Science Foundation Cooperative Agreement No. DMR-1644779 and the state of Florida.  
 464 W.F.V. acknowledges support from the UK Engineering and Physical Sciences Research Council  
 465 under Grant No. EP/P025625/1.

## 466 APPENDIX

467 Here we set out a plausible derivation of the velocity field in the normal fluid generated by a  
 468 rectilinear quantized vortex moving with steady velocity  $U$  relative to that of the normal fluid at  
 469 infinity.

470 Let the force of mutual friction per unit length of vortex be  $f$ , and let the range of this force  
 471 from the center of the vortex be  $\xi$ . We shall start by writing down the known velocity field due to  
 472 a slowly-moving solid cylinder, of radius  $a$ , in a classical fluid of viscosity  $\eta_n$  and density  $\rho_n$ ; this  
 473 field can be derived only if the nonlinear term in the Navier-Stokes equation is taken into account to  
 474 the extent assumed in the Oseen approximation [20]. We shall then make the plausible assumption  
 475 that the required velocity field at distances from the vortex considerably greater than both  $a$  and  $\xi$   
 476 is the same as that generated by the cylinder if  $a$  is chosen to lead to same drag force  $f$ .

477 The velocity field due to the moving cylinder has a simple form in the limits when the distance  $r$   
 478 from the cylinder is either much less than, or much greater than, the characteristic length  $\lambda = v_n/2U$ ,  
 479 where  $v_n = \eta_n/\rho_n$ .

480 In the former case the velocity field is given in cylindrical polar coordinates by [20]

$$481 u_r = U \cos \theta \left( 1 - \frac{C}{2} \ln \frac{r}{a} + \frac{C}{4} - \frac{Ca^2}{4r^2} \right), \quad u_\theta = -U \sin \theta \left( 1 - \frac{C}{2} \ln \frac{r}{a} - \frac{C}{4} + \frac{Ca^2}{4r^2} \right), \quad (A1)$$

482 where the parameter  $C$  is related to the force,  $f$ , by the relation

$$483 f = 2\pi \eta_n C U. \quad (A2)$$

484 It turns out, however, that this form of the “near” velocity field cannot join a satisfactory solution  
 485 for the “far” velocity field unless the parameter  $C$  is given by

$$486 C = \frac{2}{\ln(7.4\lambda/a)}. \quad (A3)$$

487 It follows from Eqs. (A1)–(A3) that

$$488 u_r = \frac{f \cos \theta}{4\pi \eta_n} \left( -\ln \frac{r}{7.4\lambda} + \frac{1}{2} - \frac{a^2}{4r^2} \right), \quad u_\theta = -\frac{f \sin \theta}{4\pi \eta_n} \left( -\ln \frac{r}{7.4\lambda} - \frac{1}{2} + \frac{a^2}{4r^2} \right). \quad (A4)$$

489 Although in the limit  $r \gg a$  these expressions for the velocity field do not depend explicitly on  
 490  $a$ , we ought to require implicitly that the force  $f$  is equal to that corresponding to the mutual friction  
 491 force,  $\alpha\kappa\rho_s U$ ; thus, we ought to check that this requirement does not lead to an unacceptable value

of  $a$ . The required value of  $a$  is in fact given by

$$a = \frac{7.4\lambda}{\exp(4\pi\rho v_n/\alpha\kappa\rho_s)}. \quad (\text{A5})$$

Using the numerical values for a temperature of 2 K set out in Sec. III(b), we find that  $a/\lambda = 3.11 \times 10^{-4}$ . The fact that this value is comparable with  $\xi$  means that it is indeed acceptable. We conclude then that the Eq. (A4) can be taken to describe the perturbation in the normal-fluid velocity field caused by a rectilinear vortex moving with velocity  $U$  relative to the normal fluid, in the near-field limit  $\lambda \gg r \gg \xi, a$ .

In the far field limit,  $r \gg \lambda$ , the velocity field produced by a moving cylinder is given by (see, for example, Mei in his Lecture Notes on Fluid Dynamics, MIT, Spring 2007)

$$u_r = -CU\left(\frac{2\pi\lambda}{r}\right)^{1/2} \exp\left(-\frac{r\theta'^2}{8\lambda}\right) + \frac{2C\lambda U}{r}, \quad (\text{A6})$$

where  $\theta' = \pi - \theta$ , and the product  $CU$  is still given in terms of  $f$  by Eq. (A2). The first term on the right-hand side of Eq. (A6) describes a wake. The second term describes a small radial flow that is required to satisfy mass continuity. As in the case of the near-field, we argue that this formula ought to describe the far velocity field for the case of the moving vortex. In describing the far velocity field it will prove convenient to use Cartesian coordinates, such that the vortex is along the  $x$  – axis and  $U$  is directed along the  $z$  axis, so that for a well-developed narrow wake

$$u_r(y, z) = -\frac{f}{\eta_n}\left(\frac{\lambda}{2\pi z}\right)^{1/2} \exp\left(-\frac{y^2}{8\lambda z}\right) + \frac{f\lambda}{\pi\eta_n(y^2 + z^2)^{1/2}}. \quad (\text{A7})$$

We can comment briefly on the physical interpretation of these results. In the near velocity field there is a simple diffusion of vorticity away from the core of the vortex; the characteristic logarithmic term arises straightforwardly from the two-dimensional diffusion equation in cylindrical polar coordinates. The existence of the velocity  $U$  is unimportant as long as the front of the diffusing region is moving at a speed greater than  $U$ . The velocity of this front is equal to  $2v_n/r$ . However, as soon as this velocity, in the transverse direction, becomes less than  $U$ , the effect of  $U$  becomes important and causes the front to swing round behind the moving cylinder or moving vortex, so giving rise to the wake. Therefore, the wake starts to form when  $2v_n/r > U$ ; i.e., when  $r > 4\lambda$ .

---

- [1] D. R. Tilley and J. Tilley, *Superfluidity and Superconductivity*, 3rd ed. (Institute of Physics Publishing, Bristol and Philadelphia, 1990).
- [2] W. F. Vinen, Mutual friction in a heat current in liquid helium II: Theory of the mutual friction, *Proc. R. Soc. London A* **242**, 493 (1957).
- [3] A. Marakov, J. Gao, W. Guo, S. W. Van Sciver, G. G. Ihss, D. N. McKinsey, and W. F. Vinen, Visualization of the normal-fluid turbulence in counterflowing superfluid  $^4\text{He}$ , *Phys. Rev. B* **91**, 094503 (2015).
- [4] J. Gao, E. Varga, W. Guo, and W. F. Vinen, Energy spectrum of thermal counterflow turbulence in superfluid helium-4, *Phys. Rev. B* **96**, 094511 (2017).
- [5] B. Mastracci and W. Guo, Exploration of thermal counterflow in helium II using particle tracking velocimetry, *Phys. Rev. Fluids* **3**, 063304 (2018).
- [6] H. E. Hall and W. F. Vinen, The rotation of liquid helium II: The theory of mutual friction in uniformly rotating helium II, *Proc. R. Soc. London A* **238**, 215 (1956).
- [7] O. C. Idowu, A. Willis, C. F. Barenghi, and D. C. Samuels, Local normal-fluid helium II flow due to mutual friction interactions with the superfluid, *Phys. Rev. B* **62**, 3409 (2000).
- [8] D. Kivotides, C. F. Barenghi, and D. C. Samuels, Triple vortex ring structure in superfluid helium II, *Science* **290**, 777 (2000).

- [9] Y. A. Sergeev, S. Wang, E. Meneguz, and C. F. Barenghi, Influence of normal fluid disturbances on interactions of solid particles with quantized vortices, *J. Low Temp. Phys.* **146**, 417 (2007).
- [10] D. R. Poole, C. F. Barenghi, Y. A. Sergeev, and W. F. Vinen, Motion of tracer particles in He II, *Phys. Rev. B* **71**, 064514 (2005).
- [11] W. F. Vinen and J. J. Niemela, Quantum turbulence, *J. Low Temp. Phys.* **128**, 167 (2002).
- [12] R. J. Donnelly and C. F. Barenghi, The observed properties of liquid helium at the saturated vapor pressure, *J. Phys. Chem. Ref. Data* **27**, 1217 (1998).
- [13] P. E. Roche, P. Diribarne, T. Didelot, O. François, L. Rousseau, and H. Willaime, Vortex density spectrum of quantum turbulence, *Europhys. Lett.* **77**, 66002 (2007).
- [14] P. E. Roche and C. F. Barenghi, Vortex spectrum in superfluid turbulence: Interpretation of a recent experiment, *Europhys. Lett.* **81**, 36002 (2008).
- [15] A. W. Baggaley and S. Laizet, Vortex line density in counterflowing He II with laminar and turbulent normal fluid velocity profiles, *Phys. Fluids* **25**, 115101 (2013).
- [16] L. Biferale, D. Khomenko, V. L'vov, A. Pomyalov, I. Procaccia, and G. Sahoo, Superfluid Helium in Three-Dimensional Counterflow Differs Strongly from Classical Flows: Anisotropy on Small Scales, *Phys. Rev. Lett.* **122**, 144501 (2019).
- [17] S. Yui, M. Tsubota, and H. Kobayashi, Three-Dimensional Coupled Dynamics of the Two-Fluid Model in Superfluid  $^4\text{He}$ : Deformed Velocity Profile of Normal Fluid in Thermal Counterflow, *Phys. Rev. Lett.* **120**, 155301 (2018).
- [18] J. Gao, W. Guo, S. Yui, M. Tsubota, and W. F. Vinen, Dissipation in quantum turbulence in superfluid  $^4\text{He}$  above 1 K, *Phys. Rev. B* **97**, 184518 (2018).
- [19] H. Adachi, S. Fujiyama, and M. Tsubota, Steady-state counterflow quantum turbulence: Simulation of vortex filaments using the full Biot-Savart law, *Phys. Rev. B* **81**, 104511 (2010).
- [20] G. K. Batchelor, *An Introduction to Fluid Dynamics* (Cambridge University Press, Cambridge, 2005).